Colloid Polym Sci 274:1109–1118 (1996)

ORIGINAL CONTRIBUTION

M. Trznadel
S. Slomkowski

Formation and morphology of latex monolayers. Computer simulation studies

Received: 30 January 1996
Accepted: 9 May 1996

Dr. M. Trznadel (✉) · S. Slomkowski
Center of Molecular
and Macromolecular Studies
Sienkiewicza 112
90-363 Lodz, Poland

Abstract The results of computer simulations of monolayers created from monodisperse latex particles are presented and discussed. Layers are characterized by the normalized coverage, *NC* (the actual coverage of the surface related to its maximum possible coverage with particles), and by the average number of neighbors, *ANN*, calculated as the number of particles being in contact with a given one and averaged over all the particles on the surface. Variable parameters used in simulations include: the rate of particles deposition, the probability of lateral movements, the probability of desorption of particles adsorbed on the surface, the probability of covalent immobilization of adsorbed particles, and the "on-sphere slip" parameter, OSS (characterizing the scattering of a falling particle on the particles being already attached to the surface). Morphology of monolayers is qualitatively characterized by relations between *ANN* and *NC*. It is shown that for all monolayers formed without adhesion (and without repulsion) between the particles adsorbed on the surface the dependence of *ANN* vs. *NC* is described by a characteristic master curve (regardless of the values of probabilities of desorption and lateral movements of particles). For the monolayers created including adhesive forces between the adsorbed particles the plots of *ANN* vs. *NC* lie above the master curve, while similar plots obtained for the layers made of particles showing various types of repulsive interactions are always placed below it. Thus, the dependencies of *ANN* vs. *NC*, derived from computer simulations, can be used for the determination of the character of the interparticle interactions in the real systems.

Key words Latex monolayers–morphology – computer simulations

Introduction

Comprehensive studies on the formation and morphology of monolayers of latex particles at interfaces and studies of properties of surfaces covered with latex monolayers are interesting not only for theoretical reasons but also because such materials are prospective in potential applications. It is of primary importance to find general laws describing the disorder-order transitions for small molecules, macromolecules, and well defined particles assembled at interfaces. There is a lot of information on the arrangements of molecules constituting building blocks of the Langmuir–Blodgett films at liquid–gas interfaces. Here, the references are given only to a few selected monographs and books collecting conference materials [1–3]. There are also reports on the studies of self-organization of macromolecules, with special attention focused on the

mono- and multi-layers of the biologically active compounds, e.g. proteins and DNA [4–10]. It is assumed that various physicochemical and biological properties of molecules arranged into two-dimensional assemblies could be different than properties of the same molecules chaotically distributed in solution.

Numerous studies on latex aggregates at interfaces concerned adsorbed particles, in some instances absorbed irreversibly [11–28]. Special attention was concentrated on relations between parameters characterizing flow of latex suspension and kinetics of particle adsorption. Recently, also in our laboratories, there were obtained monolayers of particles bound covalently to solid supports, e.g. to quartz, glass, gold, aluminum, and SiO_2 [29–33]. Our recent works include the works on the particle–particle and particle–substrate interactions and their influence on morphology of the monolayers. In the first papers we gave the examples of the controlled formation of the 2-D poly(styrene/acrolein) latex assemblies immobilized covalently on quartz [30, 32]. In this work, on the basis of computer simulation studies, we describe the relations between morphology of latex monolayers and probabilities of lateral movements of particles on the surface, particle desorption, and covalent immobilization.

The analysis of computer simulations can be useful for planning new experiments. The simulations may indicate which properties of latex particles and solid supports should be varied to obtain latex monolayers of the desired morphology. The simulations also show the limitations characteristic for the 2-D latex assemblies indicating which types of latex monolayers cannot be produced at the particular experimental conditions. The relations determined during analysis of simulations discussed in this paper may be used for the discrimination between various possible mechanisms responsible for the formation of monolayers in the real systems.

The program

The computer program written in our laboratory enables simulating of 2-D monolayers consisting of maximum 10000 monodisperse spheres on the surface of the square cell. To minimize the problems related with a limited size of the square cell the periodic boundary conditions were applied for the simulation [34].

Variable parameters determining formation of a latex monolayer include the probability of generation of spheres on the cell surface (in real system related directly to the rate of particle deposition), the probability of lateral motion of adsorbed particles, the probability of particle desorption, and the probability of immobilization of spheres on the surface (in the real systems realized, for example, by chemical bonding to the surface). Other parameters describe the particle–particle interactions. One of them, called "on-sphere slip" (OSS), reflects the possibility that a falling sphere does not need to meet directly unoccupied area to become adsorbed on the surface – the newcoming particle can slip on the attached particle and reach the surface in its nearest proximity. The model assuming the possibility that the falling sphere may roll or slip on another during its way towards the surface was introduced by Jullien and Meakin [19] and called the "ballistic model". Experimentally it was verified for large polystyrene particles (with diameters larger than 2 μm) for which, during the deposition, the movement under gravitational forces prevails over the Brownian motion [25, 26]. However, it is possible that this mechanism can characterize also the formation of layers made of soft particles for which scattering is inelastic. The "on-sphere slip" is always associated with the horizontal displacement of the newcoming sphere. The maximum value of this displacement (expressed in percent of the sphere's diameter) is taken as a quantitative measure of the OSS parameter. Thus, OSS can be varied from 0% (the new sphere must fall directly on the free surface to be adsorbed) to values slightly below 100% (in calculations we assumed $OSS_{max} = 99\%$ which corresponds to the situation when the new sphere may reach the surface even if falls almost centrally on the sphere below).

The probability of lateral movements of adsorbed particles and the probability of their desorption are affected by the interactions (attraction or repulsion) existing between the spheres on the surface. Generally, to assess these interactions it is necessary to take into account corresponding potentials of the interparticle forces for each particular system. However, in the case of short-range interactions, it is plausible to assume that at isothermal conditions both the probability of desorption (P_D) and the probability of lateral movements (P_{LM}) of particles adsorbed on the surface vary exponentially with the number of their neighbors:

$$P_D = P_{0D} \exp(-A \cdot N_N) \quad (1)$$

$$P_{LM} = P_{0LM} \exp(-A \cdot N_N) \quad (2)$$

where N_N denotes the number of spheres being in contact with the considered one, P_{0D} and P_{0LM} are, respectively, probabilities of desorption and lateral movements of isolated adsorbed particles, and A is the quantity characterizing the interaction between attached particles. N_N can vary from 0 to 6, however, for geometrical reasons for any particle with $N_N > 4$ the lateral motion becomes impossible and this restriction was included into the program.

During simulations the positions of spheres on the surface and information concerning their immobilization

were recorded. The graphical option gives the possibility for visual examination of the formation of the layer in real-time. This statistical option allows the calculation of the values of various functions characterizing the distribution of spheres on the surface. Simulations were repeated at least five times for every chosen set of parameters in order to obtain the averaged data.

Results and discussion

Maximum filling

The maximum filling of the simulation area was analyzed in order to estimate the influence of the boundary effects and to assess the necessary dimension of the simulation cell. Geometrical requirements indicate that for the maximum hexagonal packing of the square cell with spheres of the diameter D the number of spheres filling the square can be expressed by the following approximation:

$$N_{\max} \approx \frac{2}{\sqrt{3}}\left(\frac{S}{D}\right)^2 - \frac{1}{2}\left(\frac{S}{D}\right) \tag{3}$$

where S is the side of the square. The maximum value of the average number of neighbors depends on the relative size of the simulation square (S/D) in the following way:

$$ANN_{\max} = 6 - \frac{4}{N_{\max}}\left(\frac{S}{D}\right). \tag{4}$$

The surface coverage of the square cell with the monolayer consisting of N spheres is defined as:

$$C_{\text{surf}} = \frac{\pi N}{4}\left(\frac{D}{S}\right)^2 \cdot 100\% \,. \tag{5}$$

For $N = N_{\max}$ the maximum surface coverage is obtained; it is easy to notice that when $S \gg D$ the second term in formula (3) can be omitted and Eqs. (3) and (5) yield the maximum surface coverage as C_{surf} (MAX) = 90.69%.

For the given size of the simulation cell, only the spheres with certain diameters can form the hexagonally packed layer covering the whole cell surface without leaving voids. The results of computer experiments showed that the dependence of maximum coverage as the function of S/D ratio is characterized by the presence of periodical discontinuities. They occur every time when S increases to such extent that the new row of spheres can be placed on the surface. The analysis revealed that for $S/D > 20$ (corresponding to $N_{\max} = 440$ spheres) the relative deviation of simulated values from the approximate Eqs. (4) and (5) is less than 3%.

General remarks

It is reasonable to expect that for any conditions of the layer formation, regardless of the cell size, the time period necessary for obtaining a given coverage with spheres should be inversely proportional to the flux of the spheres towards the surface and to the minimum area suitable to accommodate one sphere. Thus, the normalized time (τ) making the kinetics of the layer formation independent of the flux of falling spheres and of their diameters, can be defined as follows:

$$\tau = t \cdot \text{flux} \cdot D^2 \cdot \tag{6}$$

The scaling relation given in Eq. (6) was verified in numerous simulations carried out at various conditions. It was found that for the systems differing only in the flux of particles (and/or in the particle diameter), the kinetics of the surface coverage was identical when C_{surf} was plotted vs. the normalized time. Other parameters used further for the layer characterization are the average number of neighbors (ANN) and the normalized coverage (NC) defined as $NC = C_{\text{surf}}/C_{\text{surf}}(\text{MAX})$. In several papers the morphology of two-dimensional latex assemblies was characterized by the radial distribution function $g(r)$ defined as the ratio of the average number of particles at the distance between r and $r + dr$ from a particle related to the average number of particles on the surface $2\pi r dr$ [25, 27]. The parameter ANN introduced here describes only the nearest vicinity of particles. However, as shown further, pairs of ANN and NC values may be used as simple and convenient way for discrimination between 2-D latex assemblies formed according to various mechanisms.

The initial simulations were designed for the investigations of the morphology of the layer formed without lateral movements of the spheres and without adhesion between spheres on the surface ($P_{\text{OLM}} = 0$ and $A = 0$). Data presented in Fig. 1 indicate that in the plot of ANN versus NC, regardless of the ratio between the probability of desorption (P_{OD}) and the probability of immobilization (P_{F}), all the points characterizing the simulated assemblies lie in one line. This means that the morphology of the layer is independent of the diameter of the spheres and of the probabilities of desorption and covalent immobilization. Moreover, the random desorption can be considered as a process which simply "shifts in time" the formation of a monolayer, so the morphology of monolayers formed, assuming the random desorption of spheres, is the same as the morphology obtained at the earlier time moments in processes where desorption is not involved.

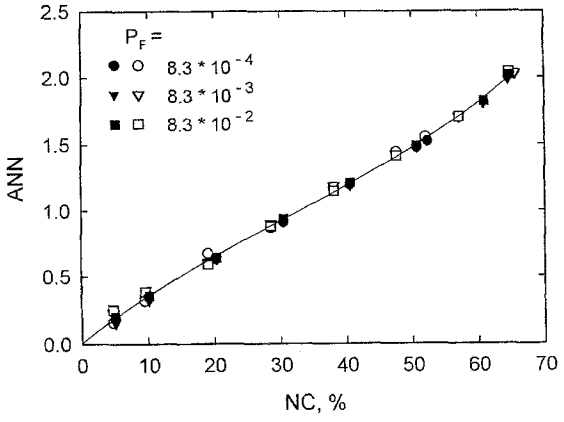

Fig. 1 Relation between the average number of neighbors (ANN) and the normalized coverage (NC) for S/D equal 20 (hollow symbols) and 80 (filled symbols). Simulation parameters: OSS = 50%; $A = 0$; $P_{0D} = 8.3 \cdot 10^{-2}$; $P_{0LM} = 0$; $P_F = 0$, $8.3 \cdot 10^{-4}$, $8.3 \cdot 10^{-3}$, and $8.3 \cdot 10^{-2}$

Effect of the on-sphere slip on the formation of the layer

The values of the OSS parameter characterize interactions between falling particles and particles attached to the layer. Elastic scattering is represented by OSS = 0% indicating that every particle falling on the one already present on the surface has to be scattered back without reaching the surface. In the case of the perfectly inelastic scattering every particle which does not fall exactly coaxially on the other one on the surface can slide on it and reach the surface nearby. The plots NC vs. τ and ANN vs. NC constructed for the system with the instantaneous immobilization (cf. Fig. 2) indicate that the inelastic scattering significantly increases the rate of the layer formation and the values of ANN for every coverage. The dependencies showing the maximum coverage vs. OSS and the maximum values of ANN vs. OSS are presented in Fig. 3. For OSS = 0% C_{surf} (MAX) = 55.5 ± 0.8% (other authors reported C_{surf} (MAX) = 54.6% [18, 28]), whereas for OSS = 99% C_{surf} (MAX) = 62.0 ± 0.8% (according to the "ballistic model" Jullien and Meakin found C_{surf} (MAX) = 61.1% [19]). The influence of the OSS parameter on ANN(MAX) is even more distinct: for OSS = 0% ANN(MAX) = 1.17 ± 0.04 whereas for OSS = 99% the maximum value of the average number of neighbors is two times higher (ANN(MAX) = 2.36 ± 0.03).

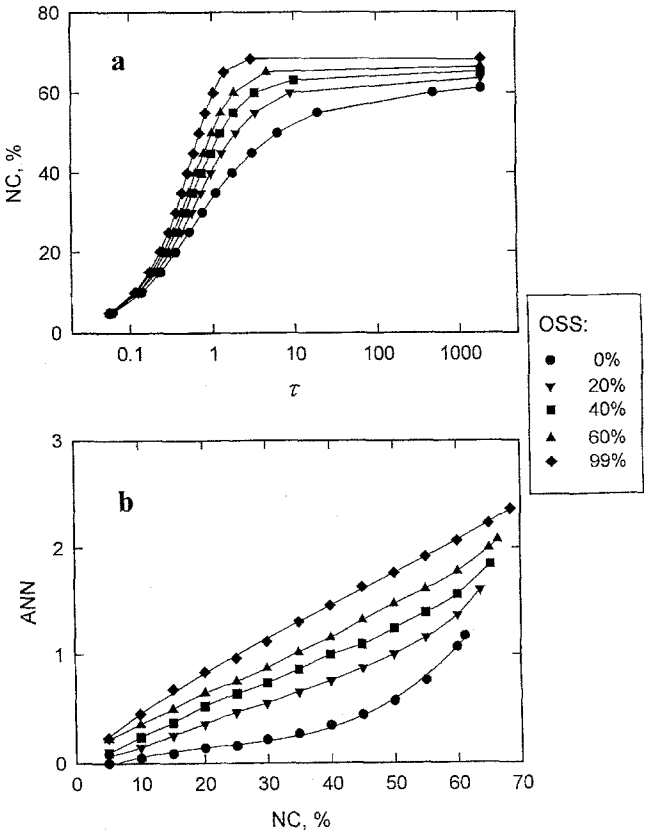

Fig. 2 Influence of the OSS parameter on the kinetics of the surface coverage (a), and on the relation between ANN and NC (b). Simulation parameters: $A = 0$; $P_{0D} = 0$; $P_{0LM} = 0$; $P_F = 1$; OSS = 0, 20, 40, 60, and 99%

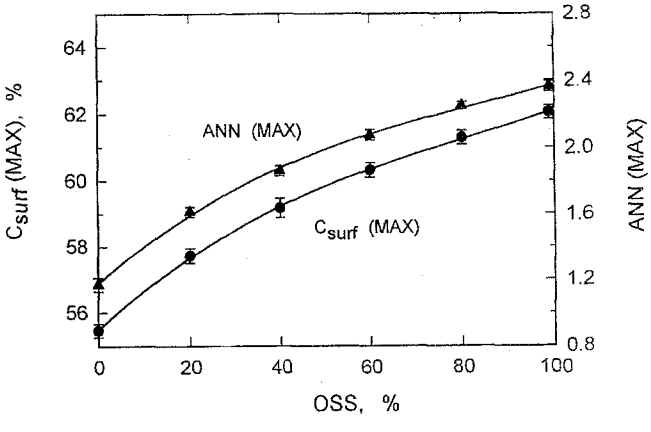

Fig. 3 Dependence of the maximum coverage (C_{surf}(MAX)) and maximum ANN (ANN(MAX)) on OSS. Simulation parameters: $A = 0$; $P_{0D} = 0$; $P_{0LM} = 0$; $P_F = 1$

The influence of lateral motion of spheres

The role of lateral motion was analyzed for systems without desorption of spheres ($P_{0D} = 0$) and without the sphere-to-sphere adhesion ($A = 0$). Simulations were carried out for various values of the OSS parameter assuming the probability of immobilization (P_F) and the probability of lateral motion (P_{0LM}) satisfying the condition $P_F + P_{0LM} = 1$. The plots ANN vs. τ and ANN vs. NC for two extreme OSS values are presented in Fig. 4 and Fig. 5

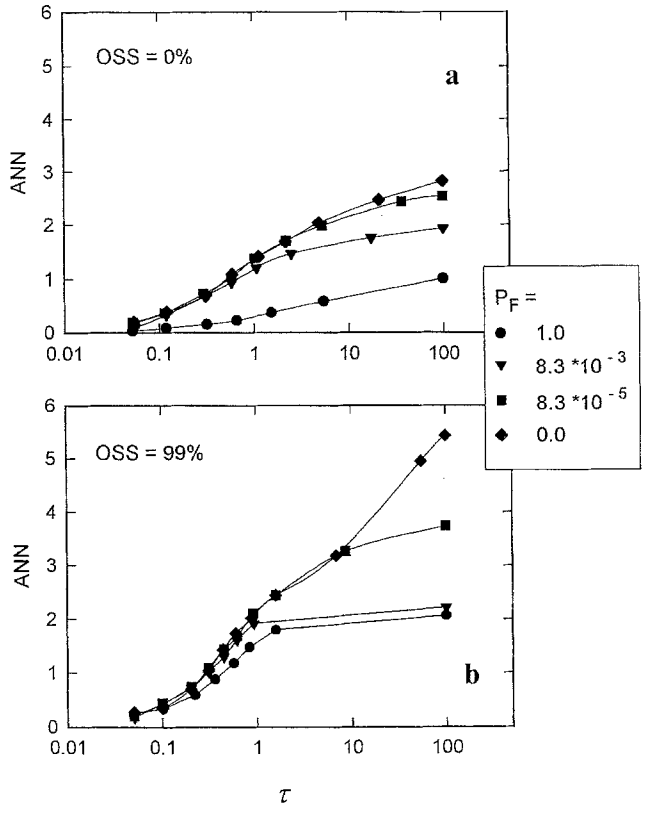

Fig. 4 Plots of ANN versus τ for OSS = 0% (a) and OSS = 99% (b). Simulation parameters: $A = 0$; $P_D = 0$; $P_F + P_{LM} = 1$; $P_F = 1$, $8.3 \cdot 10^{-3}$, $8.3 \cdot 10^{-5}$

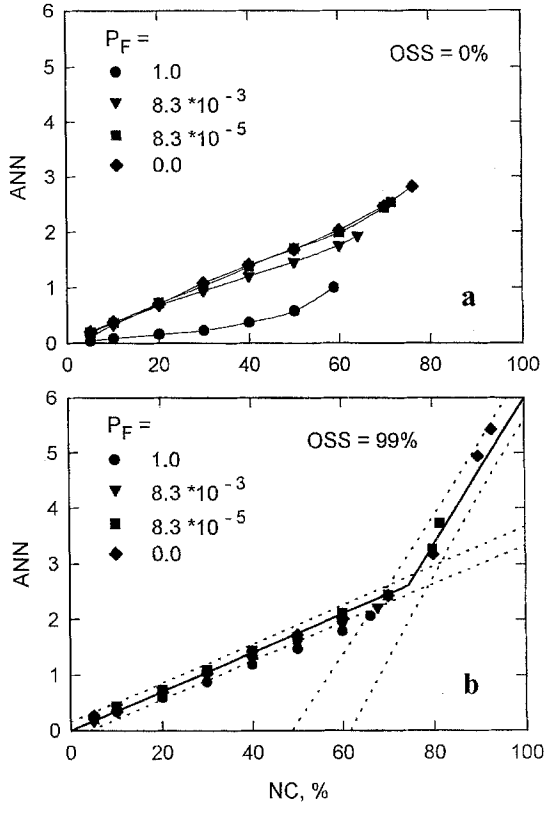

Fig. 5 Relation between ANN and NC for OSS = 0% (a) and for OSS = 99% (b). Simulation parameters: $A = 0$; $P_{OD} = 0$; $P_F + P_{OLM} = 1$; $P_F = 1$, $8.3 \cdot 10^{-3}$, $8.3 \cdot 10^{-5}$

respectively. The difference between the formation of monolayers for OSS = 0% (elastic scattering) and for OSS = 99% (perfectly inelastic scattering) is clearly manifested. For OSS = 0% the kinetic plot describing the formation of the monolayer with the instantaneous immobilization of spheres ($P_F = 1$) strays from the others. For the perfectly inelastic scattering while $\tau < 1$ the plot of ANN versus τ is only slightly dependent on the probabilities of lateral movement and on the covalent immobilization; ANN grows quickly to the values close to 2. While $\tau > 1$ the kinetics of ANN becomes significantly dependent on the probabilities of the lateral motion and on the covalent immobilization. For $P_F/P_{0LM} \geq 8.5 \cdot 10^{-5}$ the plots indicate that the growth of ANN comes to a saturation level placed well below 6. However, for systems without the covalent immobilization ($P_F/P_{0LM} = 0$) the rapid rise of ANN is observed for $\tau > 1$, suggesting that the layer formation proceeds in two steps.

The plots collected in Fig. 5 demonstrate that for all simulations with higher OSS values (regardless of the P_F and P_{0LM} values) and for some simulations with OSS = 0% (provided that P_F/P_{0LM} is sufficiently low) all the plots characterizing the relation between ANN and NC converge to the general master curve. This means that at these conditions all the assemblies show the same morphology for any given coverage of the surface. The master curve can be approximated with two straight lines and the 95% confidence interval of this approximation is marked with dashed lines. The coordinates of the intersection point are the following:

$$NC = 74.5 \pm 2.0\% \tag{7}$$

$$ANN = 2.62 \pm 0.09\,. \tag{8}$$

The two-stage process of the layer formation is visualized in Fig. 6 presenting the changes of a fragment of the simulation area during the layer formation. At the beginning ANN increases slowly with increasing NC and the spheres on the surface are distributed chaotically without any tendency for aggregation until the moment when the attachment of the additional spheres requires the rearrangement of the particles already adsorbed on the surface. The following increase of the coverage is associated with the rapid arrangement of spheres into 2-D crystal-like domains. The domains, however, are randomly oriented on the surface and their borders cannot be fitted together.

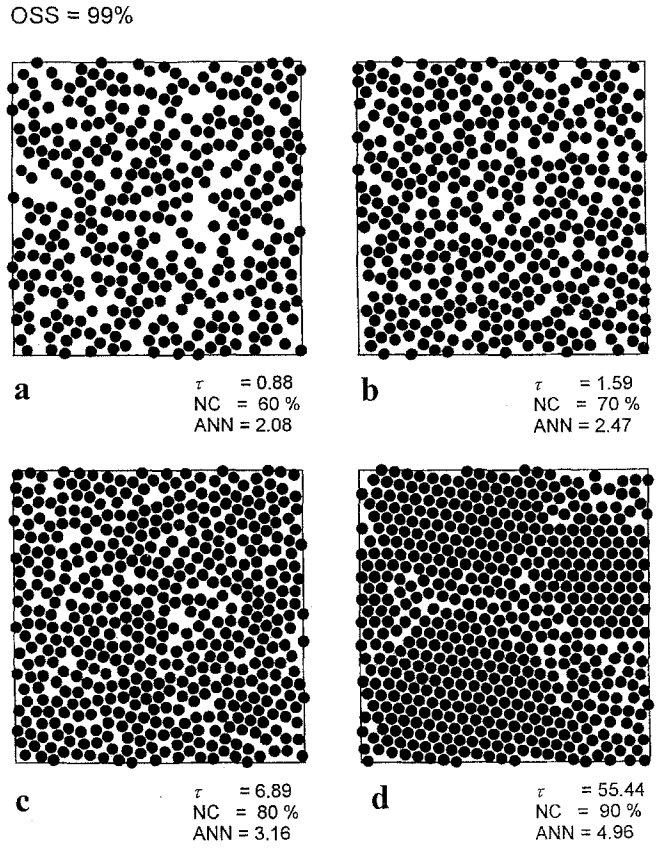

Fig. 6 Examples of simulated 2-D assemblies of spheres. Simulation parameters: $A = 0$; $P_{0D} = 0$; $P_F = 0$; $P_{0LM} = 1$; OSS = 99%

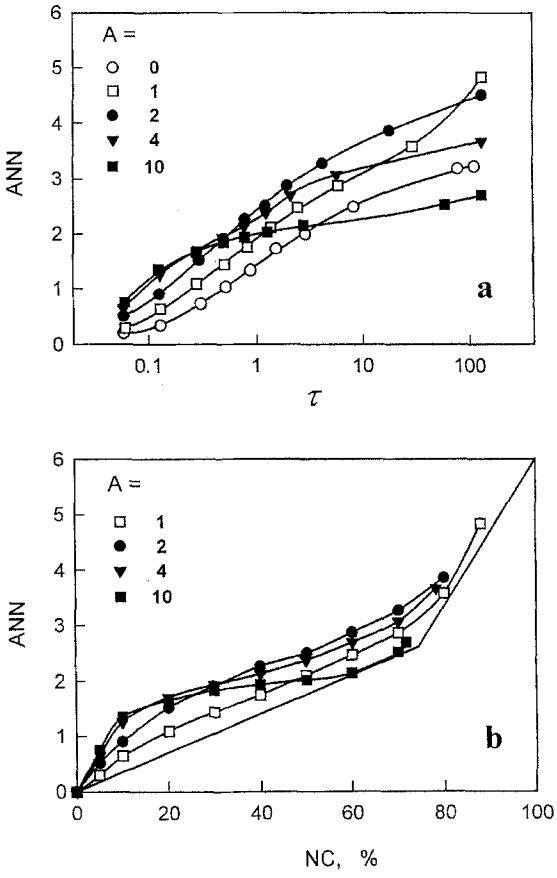

Fig. 7 Dependence of ANN on τ (a) and the relation between ANN and NC (b) for various adhesion parameters. Simulation parameters: $P_{0D} = 0$; $P_F = 0$; $P_{0LM} = 1$; OSS = 20%; $A = 1, 2, 4, 10$

That entropic effect reduces the probability of the perfect hexagonal packing of spheres on the large surface areas.

The influence of adhesion between spheres

We assumed that when adhesion between particles is involved the probability of lateral movement and the probability of desorption depend on the number of neighbors of every sphere according to Eqs. (1) and (2). This section describes how adhesion between particles affects the kinetics of the formation of 2-D layers and the morphology of created assemblies.

Systems formed including lateral movement of spheres and excluding desorption

The parameter A (cf. Eq. (2)) determining the dependence of the probability of lateral movement on the number of neighbors was varied from 0 (no adhesion) to 10. Plots of ANN versus τ, collected in Fig. 7a, indicate that initially the adhesion between particles facilitates the formation of aggregates (kinetic traces are above the curve corresponding to the systems without adhesion). However, at the later stages increased adhesion hampers further rearrangement of aggregates due to the reduced mobility of particles being in contact with several neighbors. It is important to note that for the systems with adhesion between particles the plots of ANN versus NC are always above the master curve corresponding to the zero adhesion (cf. Fig. 8b). Figure 7b also shows that for lower coverage ($NC <$ about 25%) the higher ANN values correspond to the higher adhesion parameter A. However, for higher values of NC (above 25%) there is an optimum value of A which allows attaining of the highest aggregation of spheres. Detailed calculations revealed that, for the assumed exponential dependence of the probability of lateral movements, this optimum value of the adhesion parameter is independent of the probability of immobilization (P_F) and of the probability P_{0LM} (cf. Eq. (1)) and can be approximated as $A \approx 2$.

The influence of the immobilization of spheres on morphology of the layer formed for $A = 2$ is shown in Fig. 9. In

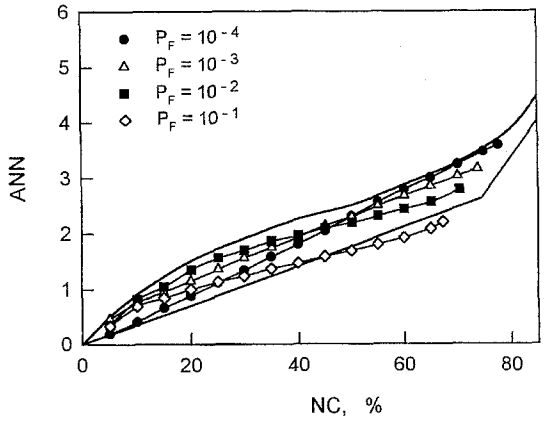

Fig. 8 Dependence of *ANN* on *NC* for various probabilities of immobilization. Simulation parameters: $P_{0D} = 0$; $A = 2$; $P_{0LM} + P_F = 1$; $P_F = 10^{-4}$, 10^{-3}, 10^{-2}, and 10^{-1}

general, the plots of *ANN* versus *NC* lie between the master curve and the curve representing the layer formed without the immobilization of spheres. The relation between *ANN* and P_F depends on the coverage of the surface: for the low coverage the higher values of P_F yield assemblies with higher *ANN*, for the high coverage this tendency is reversed. Apparently, in the systems with the high P_F probability the initially created aggregates are quickly "frozen". Later, when the coverage increases, these "frozen" structures hamper further ordering of the spheres in the layer. On the other hand, when the probability of the immobilization is low and the adhesion is not strong enough ($A \leq 2$) the formation of aggregates is reversible – they can dissolve due to the lateral mobility. In effect, the formation of large domains of the hexagonally packed spheres becomes possible. It is worth noticing that when P_F is sufficiently high (cf. the trace for $P_F = 10^{-1}$ in Fig. 8) freezing of the aggregated structures at the beginning of the formation of the layer results eventually in the lower values of *ANN* than those obtained in simulations without adhesion between spheres.

The plots presented in Fig. 8 were obtained for OSS = 20%. The simulations for other values of the OSS parameter revealed that, regardless of whether the morphology of all attached spheres was analyzed or only of those that were covalently immobilized, the variation of OSS influenced only the kinetics of the formation of the layer but not the layer morphology.

Systems formed including desorption of spheres and excluding lateral movement

The computer experiments show that in such conditions of simulations the aggregates can be constituted even at the

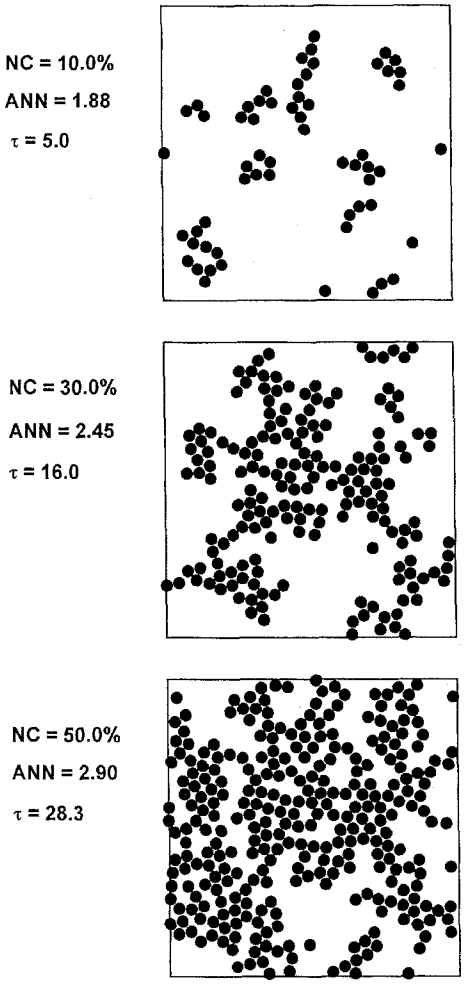

Fig. 9 Examples of 2-D assemblies of spheres. Simulation parameters: $A = 4$; $P_{0D} = 8.3 \cdot 10^{-2}$; $P_{0LM} = 0$; $P_F = 0$; OSS = 20%

early stages of the layer formation process. The simulations performed for various values of the desorption probability, P_{0D}, show that the ordering of the layer is enhanced when P_{0D} is sufficiently high so the flux of the deposition must be correlated with the flux of desorption if the layer is to be formed. When P_{0D} increases the adhesion coefficient A should also increase to maintain the relevant dependence of P_D on A, according to Eq. (1). Hence there is no distinct value of A which corresponds to the maximum ordering of particles on the surface.

Examples of the layers simulated with the adhesion coefficient $A = 4$ and for $P_{0D} = 8.33 \cdot 10^{-2}$, $P_F = 0$, $P_{0LM} = 0$, and OSS = 20% are presented in Fig. 9. It is seen that when desorption is modified by adhesion the sphere become assembled into dendrite-like aggregates.

Generally, the ability for forming aggregates in the systems with desorption modified by adhesion depends not only on the values of P_{0D} and A but also on the

relation between the rate of adsorption, probability of desorption, and probability of immobilization. The process is complex and presentation of all the dependencies exceeds the frames of this work, thus only some representative examples are shown in Fig. 10. Figure 10a illustrates the influence of the immobilization of spheres on the relation between *ANN* and *NC* (the simulations were carried out for $P_{0D} = 1/3$, $P_{0LM} = 0$, $A = 4.0$, OSS = 20%, and P_F varied from $8.33 \cdot 10^{-5}$ to $8.33 \cdot 10^{-2}$). It is seen that for the strong adhesion between particles ($A = 4$) the lower the probability of immobilization, the closer to the master curve the traces lie. It is worth noticing that, for the presented case, the structures created on the surface are the same irrespectively whether all the adsorbed particles or only those immobilized on the layer are considered. Figure 10b shows the traces of *ANN* vs. *NC* for the similar set of parameters but with the value of the OSS parameter changed to 99% (hollow symbols refer to all the adsorbed particles while the filled ones refer only to the covalently immobilized particles). We found that in this case the process of the layer formation is very unstable and maximum values of *ANN* may be high (even exceed 5) but they are attained for lower coverage (not at the end of the layer formation process). The results illustrate also that when the rate of adsorption is too high (in relation to the probability of immobilization) the adsorbed structure cannot be fixed sufficiently fast. Due to the desorption some spheres became detached and the empty space created between fixed spheres cannot be filled easily because of topological hindrances. Eventually, the space is filled, all the spheres are immobilized, and the final coverage and *ANN* become relatively high, but during the layer formation process the aggregation calculated for immobilized spheres remains at significantly lower level. It is seen that in this case the aggregation of the immobilized spheres increases with the increase of the immobilization rate to the maximum value, falling with further increase of P_F.

The calculations show that when the probability of desorption is modified by adhesion between particles, the relative coverage of the surface can reach about 80%. However, it is difficult to define the maximum value of the *ANN* parameter because the highest values are reached in the range of kinetics instabilities of the process. The eventual *ANN*, corresponding to the maximum coverage, is about 3.8 but the intermediate values may exceed 5 (cf. Fig. 12b).

Fig. 10 Relation between *ANN* and *NC*. Simulation parameters (a): $A = 4$; $P_{0D} = 0.33$; $P_{0LM} = 0$; OSS = 20%; $P_F = 8.3 \cdot 10^{-5}, 8.3 \cdot 10^{-4}, 8.3 \cdot 10^{-3}, 8.3 \cdot 10^{-2}$; (b): $A = 4$; $P_{0D} = 0.33$; $P_{0LM} = 0$; OSS = 99%; $P_F = 8.3 \cdot 10^{-5}, 8.3 \cdot 10^{-4}$

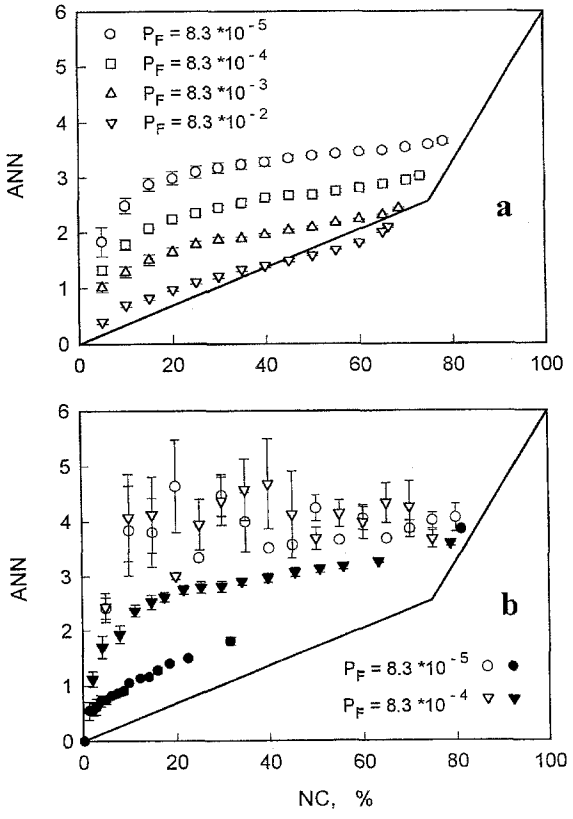

Conclusions

Several characteristic curves illustrating the dependencies of *ANN* as a function of the normalized coverage are collected in Fig. 11. The plots correspond to the layers obtained at the following conditions:

A) Lack of adhesion between adsorbed spheres; lack of their lateral mobility on the surface; elastic scattering of falling spheres from spheres adsorbed on the surface (i.e., OSS = 0%).

Fig. 11 Characteristic relations between *ANN* and *NC*. Explanation in text

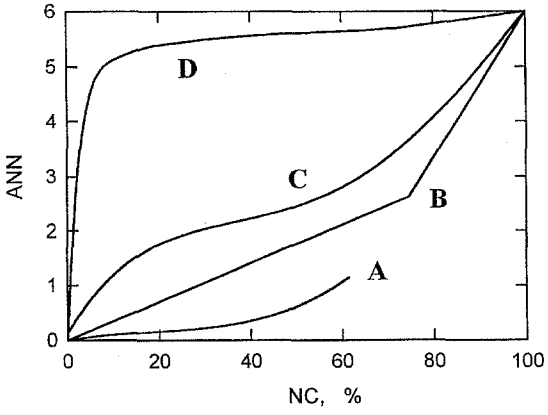

B) Lack of adhesion between adsorbed spheres; lateral mobility of spheres on the surface (or lack of scattering of falling spheres from spheres attached to the surface, i.e., OSS = 99%).

C) Lack of desorption; lack of the covalent immobilization; lateral mobility of spheres on the surface; the optimum adhesion coefficient ($A = 2.0$).

D) Development of the single hexagonal aggregate.

The curves in Fig. 11 separate several zones of typical morphologies characteristic for the layers obtained at different conditions. Points below the line A correspond to the assemblies of particles with the significantly high repulsive interactions. Points located between the lines A and B characterize layers formed from particles with short range repulsive interactions between the dropping and adsorbed particles (scattering of falling particles from particles on the surface) in the absence of their lateral movement on the surface. The layers show neither distinct order nor aggregation of particles until the point of intersection of two lines constituting the trace B. The area between the lines B and C corresponds to the layers formed from particles attracting each other and able to move on the surface. Points above the line C characterize the layers formed with particles attracting each other and being able to move on the surface or to became desorbed.

For systems without attraction between adsorbed particles, without the immobilization but with the lateral movement of adsorbed particles the layers are formed in two stages (trace B in Fig. 11). The first stage is characterized by the random arrangement of particles. During the second stage the addition of a new sphere to the layer has to be associated with the rearrangement of the whole groups of particles adsorbed on the surface. In effect, the spheres begin to create the rapidly growing, randomly oriented two-dimensional colloid crystals. The transition from the disordered to ordered layers begins for the normalized coverage $NC = 74 \pm 2\%$ and for the average number of neighbors $ANN = 2.61 \pm 0.09$.

Immobilization of particles on the surface and the decrease of the OSS parameter lead to obtaining the layers of decreased ordering of particles and decreased degree of the coverage. Attraction between the adsorbed particles and their fast immobilization on the surface create layers made of the dendrite-like assemblies. The desorption of particles, controlled by the interparticle adhesion, leads to formation of large aggregates at the beginning of the layer formation but does not enhance the arrangement of spheres when the coverage is high. To obtain the increased packing of spheres in the form of 2-D crystals the lateral motions must be involved.

The results of the simulations summarized in Fig. 11 can be used for characterization of the real systems. In the experimental practice it is possible to determine (e.g, by analysis of the microscopic pictures registered by the suitable techniques) the values of the normalized coverage and of the average number of neighbors. Location of the point, determined by values of NC and ANN in the diagram in Fig. 11, provides information on the interparticle interactions during the deposition process.

Acknowledgment The work was supported by the M. Sklodowska-Curie Fund, Grant PAN/NIST-94-169.

References

1. Allen G, Bevington JC (eds) Comprehensive polymer science. Pergamon Press, Oxford, Vol 7
2. Roberts G (ed) (1990) Langmuir–Blodgett Films. Plenum Press, New York, pp 1–425
3. Stroeve P, Balazs AC (eds) (1992) Macromolecular Assemblies in Polymeric Systems. ACS Symp Ser 493, Washington, DC, pp 1–326
4. Takeda F, Matsumoto M, Takenaka T, Fujioshi Y (1981) J Colloid Interface Sci 84:220
5. Decher G, Eßler F, Hong JD, Lowack K, Schmitt J, Lvov Y (1993) ACS Polym Prep 34(1):745
6. Subirade M, Lebulge A (1994) Thin Solid Films 243:442
7. Cheng SS, Chittur KK, Sukenik CN, Culp LA, Lewandowska K (1994) J Colloid Interface Sci 162:136
8. Minehan DS, Marx KA, Tripathy SK (1994) Macromolecules 27:777
9. Peanasky J, Schneider HM, Granick S, Kessel CR (1995) Langmuir 11:953
10. Miwa T, Yamaki M, Yoshimura H, Ebina S, Nagayama K (1995) Langmuir 11:1711
11. Ugelstad J, Berge A, Ellingsen T, Schmid R, Nilsen TN, Mørk PC, Stenstad P, Hornes E, Olsvik O (1992) Progress Polym Sci 17:87
12. Guzman RZ, Carbonell RG, Kilpatrick K (1986) J Colloid Interface Sci 114:536
13. Vincent B, Young CA, Tadros ThF (1980) J Chem Soc Faraday Trans I 76:665
14. Kallay N, Tomic M, Biskup B, Kunjasic I, Matijevic E (1987) Colloids Surf 28:185
15. Dabroś T, van de Ven TGM (1987) Physico Chem Hydrodyn 8:161
16. Varennes S, van de Ven TGM (1987) Physico Chem Hydrodyn 9:537
17. Adamczyk Z, Siwek B, Zembala M, Warszynski P (1989) J Colloid Interface Sci 130:578
18. Schaaf P, Talbot J (1989) J Chem Phys 91:4401
19. Jullien R, Meakin P (1992) J Phys A 25:L189
20. Robinson DJ, Ernshaw JC (1993) Langmuir 9:1436
21. Adamczyk Z, Szyk L, Warszynski P (1993) Colloids Surf A 75:185
22. Adamczyk Z, Siwek B, Zembala M (1993) Colloids Surf A 76:115
23. Wojtaszcyk P, Schaaf P, Senger B, Zembala M, Voegel JC (1993) J Chem Phys 99:7198
24. Adamczyk Z, Siwek B, Szyk L (1995) J Colloid Interface Sci 174:130

Colloid & Polymer Science, Vol. 274, No. 12 (1996)

25. Wojtaszczyk P, Mann EK, Senger B, Voegel JC, Schaaf P (1995) J Chem Phys 103:8285
26. Schaaf P, Wojtaszczyk P, Mann EK, Senger B, Voegel J-C, Bedeaux D (1995) J Chem Phys 102:5077
27. Mann EK, Wojtaszczyk P, Senger B, Voegel J-C, Schaaf P (1995) Europhys Lett 30:261
28. Adamczyk Z, Siwek B, Zembala M, Beloushek P (1994) Adv Colloid Interface Sci 48:151
29. Ulman A (1993) Adv Mater 5:55
30. Slomkowski S, Kowalczyk D, Trznadel M, Kryszewski M (1994) ACS Polym Prep 35(2):409
31. Freeman RG, Grabar KC, Allison KJ, Bright RM, Davis JA, Guthrie AP, Hommer MB, Jackson MA, Smith PC, Walter DG, Natan MJ (1995) Science 267:1629
32. Slomkowski S, Kowalczyk D, Trznadel M (1995) Trends Polym Sci 3:297
33. Grabar KC, Freeman RG, Hommer MB, Natan MJ (1995) Anal Chem 67:735
34. Dickinson E, Euston SR (1992) Adv Colloid Interface Sci 42:89